Distributionally robust unit commitment with an adjustable uncertainty set and dynamic demand response ☆

Ke Qing[a], Qi Huang[a,b], Yuefang Du[a,*], Lin Jiang[c], Olusola Bamisile[b], Weihao Hu[a]

[a]*Sichuan Provincial Key Lab Science and Technology of China, University of Electronic Science and Technology of China, Chengdu, China*
[b]*College of Nuclear Technology and Automation Engineering, Chengdu University of Technology, Chengdu, China*
[c]*Department of Electrical Engineering and Electronics, University of Liverpool, Liverpool, U.K.*

Abstract

To address the uncertainty of renewable energy in unit commitment, an adjustable uncertainty set of renewable energy is introduced and unit commitment is scheduled to guarantee the safe operation of the power system in this set. However, the operational risk arises when renewable energy falls out of the adjustable uncertainty set and this risk should be evaluated to determine the adjustable uncertainty set. In this paper, a distributionally robust optimization approach is proposed to calculate the risks of load shedding and renewable energy curtailment at the lower and upper bounds of the adjustable uncertainty set. After the evaluation of the operational risk, the day-ahead unit commitment with the adjustable uncertainty set is determined together with the demand response reserve in the reduction of the operational risk. In real time, the dynamic demand response is proposed to further reduce the operational risk. The proposed distributionally robust method with the dynamic demand response for dealing with the uncertainty of renewable energy is verified on the IEEE 6-bus, 30-bus, and 118-bus sys-

September 17, 2022

tems. Simulation results show that the proposed method reduces the cost of the unit commitment and the operational risk.

Nomenclature

Indices:

i Index of each subinterval.

j Index of piece cost coefficient.

t Index of each time slot.

b Index of each bus.

g Index of each unit.

l Index of each transmission line.

r Index of renewable energy (RE).

d Index of demand response (DR).

Parameters:

$\mathcal{T}$ Set of all time slots.

$\mathcal{B}$ Set of all buses.

$\mathcal{G}_b$ Set of all units at bus b.

$\mathcal{L}$ Set of all lines.

$\mathcal{R}$ Set of all REs.

$\mathcal{D}$ Set of all DRs.

p_i Probability of RE in the ith subinterval.

$F_{ls}(\cdot)/F_{rc}(\cdot)$	Function of operational risk of load shedding/RE curtailment.
$F_g^b(\cdot)$	Function of generation cost of the unit g at bus b.
$f_{g,0}^{jb}/f_{g,1}^{jb}$	jth piece cost coefficients of the unit g at bus b.
$\mathcal{P}_t^{ls}/\mathcal{P}_t^{rc}$	Ambiguity set of probability distribution (PD) of RE for calculating the risk of load shedding/RE curtailment.
$w_{t,\min}^b/w_{t,\max}^b$	Lower/upper bound of power output of RE at bus b in time slot t.
$w_t^b/\hat{w}_t^b$	Actual/forecast power output of RE at bus b in time slot t.
C_{ls}/C_{rc}	Penalty price for load shedding/RE curtailment.
C_{ld}/C_{li}	Incentive price for load decrease/increase in DR.
T	Unit commitment (UC) scheduling horizon.
$\overline{LR}_{\max}^d/\underline{LR}_{\max}^d$	Maximum load increase/decrease of DR at bus d.
β_d	Capacity of load change of DR at bus d.
SU_g^b/SD_g^b	Start-up/shut-down cost of the unit g at bus b.
MU_g^b/MD_g^b	Minimum on-time/off-time of the unit g at bus b.
IC_g^b	Minimum time of the unit g at bus b in the initial on/off state.
UR_g^b/DR_g^b	Ramp-up/ramp-down rate limit of the unit g at bus b.
$\overline{UR}_g^b/\overline{DR}_g^b$	Start-up/shut-down rate limit of the unit g at bus b.
L_g^b/U_g^b	Lower/upper bound of the power output of the unit g at bus b.
$\hat{\varepsilon}_t^b$	Forecast load at bus b in time slot t.
C_l	Capacity of transmission line l.

K_l^b	Load shift factor from bus b to line l.
K_l^r	Load shift factor from RE at bus r to line l.
K_l^d	Load shift factor from DR at bus d to line l.
$\overline{\delta}_t^b / \underline{\delta}_t^b$	Unit deviation of RE at bus b in time slot t.
N	Division number of the adjustable uncertainty set of RE.

Decision variables:

$\overline{w}_t^b / \underline{w}_t^b$	Upper/lower bound of adjustable uncertainty set at bus b in time slot t.
$\overline{M}_t^b / \underline{M}_t^b$	Deviation number of upper/lower bound of adjustable uncertainty set at bus b in time slot t.
$\overline{LR}_t^d / \underline{LR}_t^d$	Load increase/decrease of DR at bus d in time slot t.
LR_t^d	Actual usage of DR reserve at bus d in time slot t.
RE_t^r	Power generation change of RE at bus r caused by the participation of DR reserve in time slot t.
$Risk_t^b$	Operational risk at bus b in time slot t.
u_{gt}^b	Binary decision variable: "1" if unit g at bus b is started up in time slot t; "0" otherwise.
v_{gt}^b	Binary decision variable: "1" if unit g at bus b is shut down in time slot t; "0" otherwise.
y_{gt}^b	Binary decision variable: "1" if unit g at bus b is on in time slot t; "0" otherwise.
x_{gt}^b	Pre-scheduled power output of the unit g at bus b in time slot t.
a_{gt}^b	Participation factor of the unit g at bus b in time slot t.
λ_i / α	Auxiliary variables.

4

$\underline{v}_{tn}^b / \underline{s}_{gtn}^b$ Auxiliary variables.

$\underline{V}_t^b / \underline{S}_{gt}^b$ Auxiliary variables.

1. Introduction

In order to reduce the emission of greenhouse gases and achieve a clean environment, more and more renewable energy (RE) has been integrated into the power system in recent years [1]. However, the intermittency and uncertainty of RE bring lots of challenges to the safe and economic operation of power systems [2]. To meet these challenges, various methods have been proposed to deal with the uncertainty of RE in power systems [3].

Stochastic optimization approach (SOA) [4] and robust optimization approach (ROA) [5] are commonly adopted to deal with the uncertainty of RE in power systems. SOA generates scenarios of RE based on the predefined probability distribution (PD) of RE, and these scenarios are taken into account in the energy scheduling of power systems [6]. Different probability distributions (PDs), such as normal distribution [7], Weibull distribution [8], and truncated versatile distribution [9], are adopted to describe the uncertainty of RE in SOA. In [10], a two-stage model is proposed to minimize the expected cost of unit commitment (UC) with the uncertainty of wind power based on the Weibull distribution. However, it is usually difficult to obtain the accurate PD of RE in practice [11], and the performance of the SOA will be affected when the RE deviates from the predefined PD [12]. In comparison with the SOA, the ROA does not rely on the PD [13]. It uses a deterministic uncertainty set, which can be constructed based on historical data in practice, to describe the uncertainty of RE [14]. The ROA can guarantee the feasibility of the solution for all realizations in the uncertainty set since it has taken into account the worst scenario [15]. Jiang et al. [16] minimize the cost of UC under the worst wind power output scenario within its maximum uncertainty set. Due to the use of the maximum uncertainty set to describe the uncertainty of RE and the consideration of the worst-case scenario, the solution obtained by the ROA is conservative with more economic cost to guarantee its feasibility in the maximum uncertainty set [17].

To deal with the conservativeness of the ROA, Zhao et al. [18] propose to combine the SOA and the ROA to schedule the UC. It introduces a weight between the expected operation cost of the SOA and the worst-case operation cost of the ROA, and the normal distribution is assumed to describe the

uncertainty of RE. Besides, a distributionally robust optimization approach (DROA) which considers both the probabilistic information and the range of the uncertainty set is proposed [19]. The DROA usually constructs an ambiguity set to describe the uncertainty and immunizes the energy scheduling strategies of the power system against all PDs in the ambiguity set. In contrast with the need of an accurate PD in the SOA, the ambiguity set in the DROA can be constructed by the statistical properties of historical data, such as mean and variance [20]. In the work of Zheng et al. [21], DROA constructs a PD set based on the moment information of historical data of wind power, and the UC cost is minimized under the worst-case PD. Xiong et al. [22] propose a two-stage optimization model to schedule the UC considering the wind power uncertainty, and it demonstrates that the DROA is less conservative than the ROA.

To reduce the conservativeness of ROA while present an interval of RE in which the safe operation of power system is guaranteed, an adjustable uncertainty set is introduced to address the uncertainty of RE in UC and it is a subset of the maximum uncertainty set of RE [23]. Wang et al. [24] determine the energy scheduling of UC and the adjustable uncertainty set with the constraints that the safety of the system operation is guaranteed within this set. However, the approach of adjustable uncertainty set brings the operational risks of load shedding and RE curtailment when the RE falls out of the adjustable uncertainty set. This risk should be taken into account when determining the adjustable uncertainty set [25]. In [26], the adjustable uncertainty set is optimized to make a trade-off between the reduction of the conservativeness of ROA and the increase of the operational risk, and it is proved that the adjustable uncertainty set helps reduce the cost of UC.

While RE is largely integrated into the power system and brings great challenges to the system, different technologies, such as the energy storage [27], power to power [28], and demand response (DR) [29], can also be used to deal with this problem. Pozo et al. [30] propose to install battery storages as reserve devices for the compensation of the wind power uncertainty in UC. In our previous work [31], a static DR program and the adjustable uncertainty set are combined to tackle the uncertainty of RE. The operational risk corresponding to the adjustable uncertainty set is taken into account and the DR reserve is scheduled to reduce this operational risk.

In this paper, a UC scheduling with the adjustable uncertainty set and the dynamic DR program is proposed to reduce the conservativeness of the ROA and improve the economy of the power system. The uncertainty of RE

is described by an adjustable uncertainty to reduce the conservativeness of using the maximum uncertainty set. In comparison with current research work that the DROA is applied directly in minimization of UC cost [32], a DROA is proposed to evaluate the operational risk of the adjustable uncertainty set in this paper. Instead of using a static DR program in our previous paper [31], a dynamic DR program that can fully utilize the capacity of the DR is proposed to reduce the operational risk of the adjustable uncertainty set. The day-ahead UC scheduling and the dynamic DR dispatch are formulated as a mixed integer nonlinear programming (MINLP) problem and the linear programming (LP) problem, respectively. Various algorithms are proposed to solve the MINLP problem, such as heuristic algorithms [33] including genetic algorithm [34], particle swarm optimization algorithm [35], lightning search algorithm [36] and bacterial foraging optimization algorithm [37], and mathematical programming including lagrangian relaxation [38], column-and-constraint generation method [39] and benders decomposition [40]. In this paper, auxiliary variables and constraints are introduced to transform the original MINLP problem into a mixed integer linear programming (MILP) problem. Finally, the MILP problem and the LP problem are solved by the Gurobi solver [41]. In summary, the major contributions of this paper are listed below:

1) Based on the historical data of RE, the DROA is proposed to evaluate the operational risk of the adjustable uncertainty set. The DROA constructs an ambiguity set of PDs of RE and calculates the operational risk under the worst-case PD. Based on the operational risk of a series of bounds of the adjustable uncertainty set, the operational risk curves are obtained by the piecewise linearization method.

2) The UC problem with the consideration of the adjustable uncertainty set and the DR program is formulated to reduce the operation cost and the operational risk. In this UC problem, the safe operation of the power system is guaranteed within the adjustable uncertainty set, and the operational risk caused by the introduction of the adjustable uncertainty set is evaluated by the operational risk curves.

3) A dynamic scheduling model of the DR reserve is proposed in real-time operation to reduce the operational risk brought by the introduction of the adjustable uncertainty set. Specifically, the remaining capacity of the DR reserve is updated based on the actual usage of the DR reserve

at each time slot, and the DR reserve is rescheduled for the following time slots. In this way, the DR reserve can be effectively utilized to reduce the operational risk.

The rest of this paper is organized as follows. The proposed DROA for the calculation of the operational risk is presented in Section 2. The problem of UC with the consideration of the adjustable uncertainty set and the dynamic DR program is formulated in Section 3. Section 4 gives the solution methodology. Simulation results are presented in Section 5 and conclusions are drawn in Section 6.

2. Operational risk based on a distributionally robust approach

In order to address the uncertainty of RE in UC, an adjustable uncertainty set is introduced in this paper. This set is a subset of the maximum uncertainty set of RE and the safe operation of the power system is guaranteed in this adjustable uncertainty set. The constraints for the safe operation of the power system will be introduced in the next section. As shown in Fig. 1, $[\underline{w}_t^b, \overline{w}_t^b]$ denotes the adjustable uncertainty set and $[w_{t,\min}^b, w_{t,\max}^b]$ denotes the maximum uncertainty set of RE. $w_{t,\min}^b$ and $w_{t,\max}^b$ represent the minimum and maximum power outputs of RE, respectively. $\hat{w}_t^b$ denotes the forecast value of RE generation with $\underline{w}_t^b \leq \hat{w}_t^b \leq \overline{w}_t^b$. Since the adjustable uncertainty set is a subset of the maximum uncertainty set, the operational risks of load shedding and RE curtailment will appear when RE falls out of the adjustable uncertainty set, i.e. falls in $[w_{t,\min}^b, \underline{w}_t^b]$ and $[\overline{w}_t^b, w_{t,\max}^b]$. In this section, a DROA that considers the worst-case PD of RE is proposed to evaluate the operational risk. Firstly, the ambiguity set of PDs of RE is constructed based on historical data. With the ambiguity set, mathematical models of the operational risks at the bounds of the adjustable uncertainty set are formulated. Then, the dualization and linearization of these mathematical models are introduced to calculate the operational risks at the bounds of the adjustable uncertainty set.
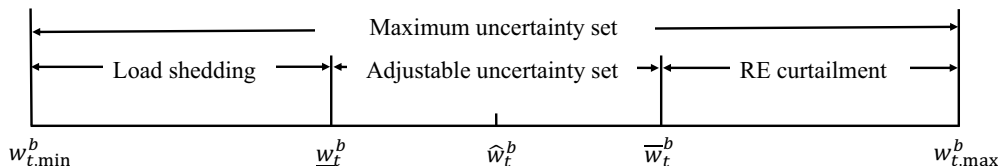

Figure 1: Adjustable uncertainty set

8

2.1. Mathematical formulation of operational risk

As shown in Fig. 2, for a certain lower bound $\underline{w}_t^b$ of the adjustable uncertainty set $[\underline{w}_t^b, \overline{w}_t^b]$, the maximum uncertainty set $\mathrm{W} = [w_{t,\min}^b, w_{t,\max}^b]$ is divided into m + 1 subintervals, i.e. $\mathrm{W}_1, \mathrm{W}_2, \ldots, \mathrm{W}_i, \ldots, \mathrm{W}_{m+1}$ with $\mathrm{W}_1 \cup \mathrm{W}_2 \cup \cdots \cup \mathrm{W}_m = [w_{t,\min}^b, \underline{w}_t^b]$ and $\mathrm{W}_{m+1} = [\underline{w}_t^b, w_{t,\max}^b]$. Based on historical data, the ambiguity set of PDs of RE is constructed as

$$
\mathcal{P}_t^{ls} = \left\{ \mathbb{P}_t \middle| \begin{array}{c} \mathbb{E}_{\mathbb{P}_t}(w_t^b) = \hat{w}_t^b \\ \mathbb{P}_t\{w_t^b \in \mathrm{W}_i\} = p_i, i = 1, 2, \ldots, \mathrm{m}, \mathrm{m} + 1 \\ \sum_{i=1}^{m+1} p_i = 1 \end{array} \right\} \tag{1}
$$

where p_i denotes the probability of RE in the ith subinterval, and the sum of the probabilities of m + 1 subintervals is 1.
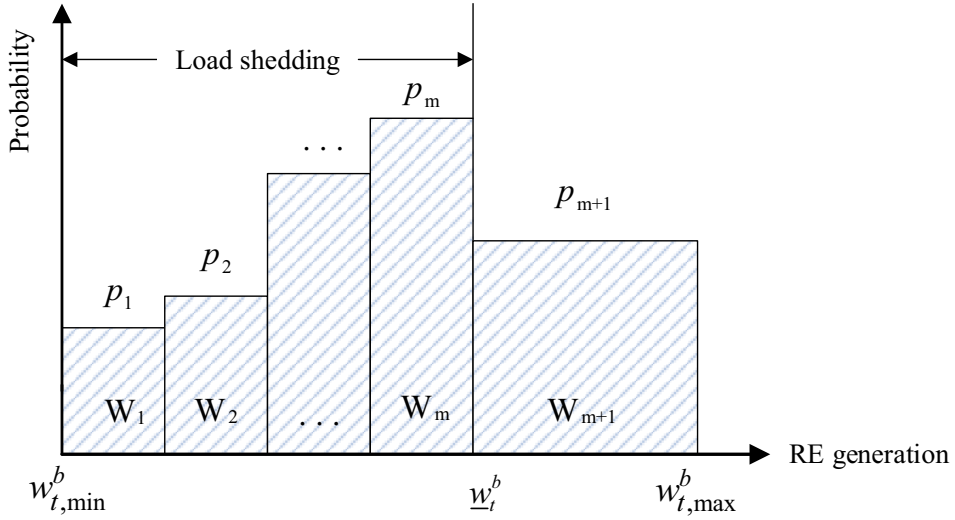

Figure 2: Probabilistic information of the ambiguity set

Considering the worst-case PD in the ambiguity set, the operational risk of load shedding at the lower bound of the adjustable uncertainty set is calculated by

$$
F_{ls}(\underline{w}_t^b) = \max_{\mathbb{P}_t \in \mathcal{P}_t^{ls}} \int_{\mathrm{W}} C_{ls}(\underline{w}_t^b - w_t^b)^+ \mathbb{P}(\mathrm{d}w_t^b) \tag{2a}
$$

9

$$s.t. \int_{\mathrm{W}} \mathrm{I}_i \mathbb{P}(\mathrm{d}w_t^b) = p_i, i = 1, 2, \ldots, \mathrm{m}, \mathrm{m}+1 \tag{2b}$$

$$\int_{\mathrm{W}} w_t^b \mathbb{P}(\mathrm{d}w_t^b) = \hat{w}_t^b \tag{2c}$$

where C_{ls} denotes the penalty price for load shedding. $(\underline{w}_t^b - w_t^b)^+ = \max\{\underline{w}_t^b - w_t^b, 0\}$, which means that there is a risk of load shedding when the actual power output of RE is less than the lower bound of the adjustable uncertainty set. In equation (2b), $\mathrm{I}_i = 1$ when $w_t^b \in \mathrm{W}_i$, otherwise $\mathrm{I}_i = 0$. Equation (2c) indicates that the expected value of RE is equal to the forecast value.

Similarly, based on historical data, the ambiguity set $\mathcal{P}_t^{rc}$ for the calculation of RE curtailment is constructed. The maximum uncertainty set $[w_{t,\min}^b, w_{t,\max}^b]$ is divided into m + 1 subintervals with $\mathrm{W}_1 \cup \mathrm{W}_2 \cup \cdots \cup \mathrm{W}_m = [\overline{w}_t^b, w_{t,\max}^b]$ and $\mathrm{W}_{\mathrm{m}+1} = [w_{t,\min}^b, \overline{w}_t^b]$. The operational risk of RE curtailment at the upper bound of the adjustable uncertainty set is formulated as

$$F_{rc}(\overline{w}_t^b) = \max_{\mathbb{P}_t \in \mathcal{P}_t^{rc}} \int_{\mathrm{W}} C_{rc}(w_t^b - \overline{w}_t^b)^+ \mathbb{P}(\mathrm{d}w_t^b) \tag{3a}$$

$$s.t. \int_{\mathrm{W}} \mathrm{I}_i \mathbb{P}(\mathrm{d}w_t^b) = p_i, i = 1, 2, \ldots, \mathrm{m}, \mathrm{m}+1 \tag{3b}$$

$$\int_{\mathrm{W}} w_t^b \mathbb{P}(\mathrm{d}w_t^b) = \hat{w}_t^b \tag{3c}$$

where C_{rc} denotes the penalty price for RE curtailment. $(w_t^b - \overline{w}_t^b)^+ = \max\{w_t^b - \overline{w}_t^b, 0\}$, which means that there is a risk of RE curtailment when the actual power output of RE is larger than the upper bound of the adjustable uncertainty set.

2.2. Dualization and linearization of operational risk

Since all the distributions in the ambiguity set $\mathcal{P}_t^{ls}$ are considered in (2), it is an infinite dimensional linear optimization problem that cannot be solved directly by existing solvers. By introducing dual variables $\lambda_i, i = 1, 2, \ldots, \mathrm{m}, \mathrm{m}+1$ and α, the optimization problem (2) is converted to a solvable finite dimensional linear optimization problem as follows:

$$F_{ls}(\underline{w}_t^b) = \min \sum_{i=1}^{\mathrm{m}+1} \lambda_i p_i + \alpha \hat{w}_t^b \tag{4a}$$

10

$$s.t. - C_{ls}(\underline{w}_t^b - w_t^b)^+ + \sum_{i=1}^{m+1} \lambda_i I_i + \alpha w_t^b \geq 0, \forall w_t^b \in W \qquad (4b)$$

Enumerating the constraints for each sub-interval $W_i \subseteq W, i = 1, 2, \ldots, m+1$, the optimization problem (4) is further transformed into

$$F_{ls}(\underline{w}_t^b) = \min \sum_{i=1}^{m+1} \lambda_i p_i + \alpha \hat{w}_t^b \qquad (5a)$$

$$s.t. - C_{ls}(\underline{w}_t^b - w_t^b) + \lambda_i + \alpha w_t^b \geq 0, \forall w_t^b \in W_i, i = 1, 2, ..., m \qquad (5b)$$

$$\lambda_i + \alpha w_t^b \geq 0, \forall w_t^b \in W_i, i = m + 1 \qquad (5c)$$

By substituting w_t^b with the lower and upper bounds of the sub-interval $W_i \subseteq W, i = 1, 2, \ldots, m + 1$, the optimization problem (5) can be solved directly by linear programming (LP). With the calculation of a series of certain lower bounds of adjustable uncertainty set, the operational risk curve of load shedding can be plotted and approximated by the piecewise linearization method [26].

Same as the dualization of load shedding risk, the calculation of RE curtailment risk is presented as follows:

$$F_{rc}(\overline{w}_t^b) = \min \sum_{i=1}^{m+1} \lambda_i p_i + \alpha \hat{w}_t^b \qquad (6a)$$

$$s.t. - C_{rc}(w_t^b - \overline{w}_t^b) + \lambda_i + \alpha w_t^b \geq 0, \forall w_t^b \in W_i, i = 1, 2, ..., m \qquad (6b)$$

$$\lambda_i + \alpha w_t^b \geq 0, \forall w_t^b \in W_i, i = m + 1 \qquad (6c)$$

After calculating the RE curtailment risks at a series of the upper bounds of the adjustable uncertainty set, the RE curtailment risk curve is obtained by the piecewise linearization method.

Notably, although the proposed method considers the worst-case PD in the ambiguity set, it does not require the knowledge of the exact worst-case PD in the evaluation of the operational risk with the dualization.

3. Unit commitment with adjustable uncertainty set and demand response reserve

In this paper, an adjustable uncertainty set is introduced to address the uncertainty of RE in UC. Since the adjustable uncertainty set brings the risk

of load shedding or RE curtailment when the actual RE generation falls out of the adjustable uncertainty set, the DR reserve is introduced to reduce the operational risk. In this section, the problem of UC with the consideration of adjustable uncertainty set and DR reserve is formulated.
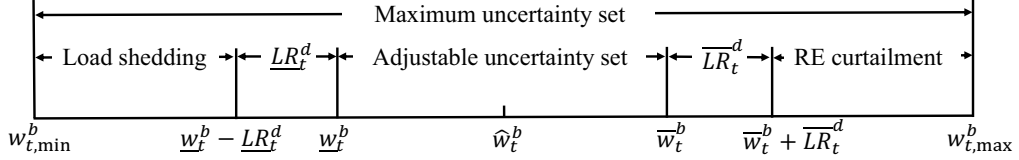

Figure 3: Adjustable uncertainty set with DR reserve

3.1. Participation of demand response

The amount of DR reserve of load increase and load decrease is limited at each time slot and the entire time horizon. The constraints are presented as

$$0 \leq \overline{LR}_t^d \leq \overline{LR}_{\max}^d \tag{7a}$$

$$0 \leq \underline{LR}_t^d \leq \underline{LR}_{\max}^d \tag{7b}$$

$$\sum_{t \in \mathcal{T}} \overline{LR}_t^d \leq \beta_d \tag{7c}$$

$$\sum_{t \in \mathcal{T}} \underline{LR}_t^d \leq \beta_d \tag{7d}$$

where inequalities (7a) and (7b) indicate the limits of DR reserve of load increase $\overline{LR}_t^d$ and load decrease $\underline{LR}_t^d$, respectively. Inequalities (7c) and (7d) represent the capacity limits of DR reserve during the whole horizon [42].

As shown in Fig. 1, the operational risk of the adjustable uncertainty set without considering the DR reserve is defined as

$$Risk_t^b = \max\{F_{ls}(\underline{w}_t^b), F_{rc}(\overline{w}_t^b)\} \tag{8}$$

Comparing Fig. 3 with Fig. 1, DR reserve can decrease the load to reduce the risk of load shedding and increase the load to reduce the risk of RE curtailment. The operational risk of the adjustable uncertainty set with the consideration of DR reserve is presented as

$$Risk_t^b = \max\{F_{ls}(\underline{w}_t^b - \underline{LR}_t^d), F_{rc}(\overline{w}_t^b + \overline{LR}_t^d)\} \tag{9}$$

12

Users will be rewarded for participating in the DR, and this reward is calculated by

$$DR_{\text{cost}} = C_{ld}\underline{LR}_t^d + C_{li}\overline{LR}_t^d \tag{10}$$

where C_{ld} and C_{li} are the incentive prices for load decrease and load increase in DR reserve, respectively.

3.2. Problem formulation of unit commitment considering adjustable uncertainty set and demand response reserve

In this subsection, the mathematical model of UC considering adjustable uncertainty set and DR reserve is presented.

3.2.1. Constraints
1) States of units

The constraints for the states of units are presented as: $\forall g \in \mathcal{G}_b, \forall b \in \mathcal{B}, \forall t \in \mathcal{T}$

$$-y_{g(t-1)}^b + y_{gt}^b - y_{gk}^b \leq 0, \forall k \in [t+1, \min\{t + MU_g^b - 1, T\}] \tag{11a}$$

$$y_{g(t-1)}^b - y_{gt}^b + y_{gk}^b \leq 1, \forall k \in [t+1, \min\{t + MD_g^b - 1, T\}] \tag{11b}$$

$$y_{gt}^b = y_{g1}^b, t \in [1, IC_g^b] \tag{11c}$$

$$-y_{g(t-1)}^b + y_{gt}^b - u_{gt}^b \leq 0 \tag{11d}$$

$$y_{g(t-1)}^b - y_{gt}^b - v_{gt}^b \leq 0 \tag{11e}$$

$$u_{gt}^b, v_{gt}^b, y_{gt}^b \in \{0,1\} \tag{11f}$$

where equations (11a) and (11b) indicate that the on/off states of the unit g are constrained by the minimum on-time MU_g^b and the minimum off-time MD_g^b. Equation (11c) indicates the minimum time for which units should stay in the initial on/off states due to the minimum up/down-time of units confined in the previous scheduling horizon. IC_g^b denotes the minimum time of the unit g at bus b in the initial on/off states. Equations (11d) and (11e) indicate the start-up and shut-down operations of units, respectively. Equation (11f) indicates that u_{gt}^b, v_{gt}^b and y_{gt}^b are binary decision variables. Binary decision variable u_{gt}^b : "1" if unit g at bus b is started up in time slot t; "0" otherwise. Binary decision variable v_{gt}^b : "1" if unit g at bus b is shut

down in time slot t; "0" otherwise. Binary decision variable y_{gt}^b: "1" if unit g at bus b is on in time slot t; "0" otherwise.

2) Power balance

Due to the advantage of computational tractability, the affinely adjustable scheme of UC is adopted in this paper [43]. In this scheme, the actual power outputs of the units are the affine functions of the forecast error of RE: $\forall g \in \mathcal{G}_b, \forall b \in \mathcal{B}, \forall t \in \mathcal{T}, \forall w_t^b \in [\underline{w}_t^b, \overline{w}_t^b]$

$$p_{gt}^b = x_{gt}^b + a_{gt}^b \sum_{b \in \mathcal{B}} (\hat{w}_t^b - w_t^b) \tag{12}$$

where x_{gt}^b denotes the pre-scheduled power output of the unit g at bus b in time slot t. a_{gt}^b denotes the participation factor of the unit g at bus b in time slot t. $\hat{w}_t^b$ denotes the forecast value of RE and w_t^b denotes the actual power output of RE. Under the affinely adjustable scheme of UC, the units are assumed to regulate their power outputs in a proportion a_{gt}^b of the forecast error of RE within the adjustable uncertainty set in real-time operation to guarantee the power balance.

To ensure the power balance, the sum of the generator power outputs x_{gt}^b and the forecast RE generation $\hat{w}_t^b$ is equal to the forecast load $\hat{\varepsilon}_t^b$: $\forall g \in \mathcal{G}_b, \forall b \in \mathcal{B}, \forall t \in \mathcal{T}$

$$\sum_{b \in \mathcal{B}} \sum_{g \in \mathcal{G}_b} (x_{gt}^b - a_{gt}^b \sum_{b \in \mathcal{B}} (\hat{\varepsilon}_t^b - \hat{w}_t^b)) = 0 \tag{13}$$

$$0 \leq a_{gt}^b \leq y_{gt}^b \tag{14}$$

$$\sum_{b \in \mathcal{B}} \sum_{g \in \mathcal{G}_b} a_{gt}^b = 1 \tag{15}$$

3) Safe operation of power system

As shown in constraints (16a)-(16f), the safe operation of the power system is guaranteed in the adjustable uncertainty set $[\underline{w}_t^b, \overline{w}_t^b]$: $\forall g \in \mathcal{G}_b, \forall b \in \mathcal{B}, \forall l \in \mathcal{L}, \forall t \in \mathcal{T}, \forall w_t^b \in [\underline{w}_t^b, \overline{w}_t^b], \forall LR_t^d \in [-\underline{LR}_t^d, \overline{LR}_t^d]$

$$p_{gt}^b - p_{g(t-1)}^b \leq (2 - y_{g(t-1)}^b - y_{gt}^b)\overline{UR}_g^b + (1 + y_{g(t-1)}^b - y_{gt}^b)UR_g^b \tag{16a}$$

$$p_{g(t-1)}^b - p_{gt}^b \leq (2 - y_{g(t-1)}^b - y_{gt}^b)\overline{DR}_g^b + (1 - y_{g(t-1)}^b + y_{gt}^b)DR_g^b \tag{16b}$$

$$p_{gt}^b - L_g^b y_{gt}^b \geq 0 \tag{16c}$$

14

$$p_{gt}^b - U_g^b y_{gt}^b \leq 0 \qquad (16d)$$

$$\sum_{b \in \mathcal{B}} K_l^b \left(\sum_{g \in \mathcal{G}_b} p_{gt}^b - (\hat{\varepsilon}_t^b - w_t^b) \right) + \sum_{r \in \mathcal{R}} RE_t^r K_l^r - \sum_{d \in \mathcal{D}} LR_t^d K_l^d + C_l \geq 0 \quad (16e)$$

$$\sum_{b \in \mathcal{B}} K_l^b \left(\sum_{g \in \mathcal{G}_b} p_{gt}^b - (\hat{\varepsilon}_t^b - w_t^b) \right) + \sum_{r \in \mathcal{R}} RE_t^r K_l^r - \sum_{d \in \mathcal{D}} LR_t^d K_l^d - C_l \leq 0 \quad (16f)$$

where equations (16a) and (16b) are the constraints for the ramp-up and ramp-down rates of the units. $\overline{UR}_g^b$ and $\overline{DR}_g^b$ denote the start-up and shut-down rate limits of the unit g at bus b, respectively. UR_g^b and DR_g^b denote the ramp-up and ramp-down rate limits of the unit g at bus b, respectively. Equations (16c) and (16d) are the constraints for the power outputs of the units. L_g^b and U_g^b denote the lower and upper limits of the power output of the unit g at bus b, respectively. With the consideration of the DR reserve, the limits of the transmission line capacity are described in equations (16e) and (16f). K_l^b represents the power flow transfer factor at bus b to line l. K_l^r represents the power flow transfer factor of the power generation change of RE at bus r to line l. K_l^d represents the power flow transfer factor of DR reserve at bus d to line l. Since RE_t^r is the power generation change of RE caused by the DR LR_t^d, RE_t^r is equal to LR_t^d.

3.2.2. Complete model of unit commitment

To minimize the total cost of UC which includes the operation costs of the units, the operational risks of load shedding and RE curtailment, and the rewards for users to participate in DR [44], the UC problem is formulated as

$$\min_{\boldsymbol{u},\boldsymbol{v},\boldsymbol{y},\boldsymbol{x},\boldsymbol{a},\boldsymbol{w},\boldsymbol{r}} \left\{ \sum_{t \in \mathcal{T}} \sum_{b \in \mathcal{B}} \sum_{g \in \mathcal{G}_b} \underbrace{SU_g^b u_{gt}^b + SD_g^b v_{gt}^b + F_g^b(y_{gt}^b, x_{gt}^b)}_{\text{Operation costs of the units}} \right.$$

$$\left. + \underbrace{Risk_t^b}_{\text{Operational risk}} + \underbrace{C_{ld} \underline{LR}_t^d + C_{li} \overline{LR}_t^d}_{\text{Rewards for users}} \right\} \qquad (17a)$$

$$s.t. \; \forall g \in \mathcal{G}_b, \forall b \in \mathcal{B}, \forall l \in \mathcal{L}, \forall t \in \mathcal{T}, \forall w_t^b \in [\underline{w}_t^b, \overline{w}_t^b], \forall LR_t^d \in [-\underline{LR}_t^d, \overline{LR}_t^d]$$

$$(7a) - (7d), (9), (11a) - (16f) \qquad (17b)$$

where $\boldsymbol{u}$, $\boldsymbol{v}$, and $\boldsymbol{y}$ denote the binary decision variables of start-up, shut-down, and on/off states of units, respectively. $\boldsymbol{x}$, $\boldsymbol{a}$ denote the generation decisions and participation factors of units, respectively. $\boldsymbol{w}$ denotes the vector of

lower and upper bounds of the adjustable uncertainty set. $\boldsymbol{r}$ denotes the day-ahead scheduling of DR reserve. SU_g^b and SD_g^b denote the start-up and shut-down costs of the unit g at bus b, respectively. The generation cost function $F_g^b(y_{gt}^b, x_{gt}^b)$ is expressed as a J-piece piecewise linear function [45], which satisfies $F_g^b(y_{gt}^b, x_{gt}^b) \geq f_{g,0}^{jb} y_{gt}^b + f_{g,1}^{jb} x_{gt}^b, j = 1, 2, \ldots, J$. $f_{g,0}^{jb}$ and $f_{g,1}^{jb}$ denote the jth piece cost coefficients of the unit g at bus b.

3.3. Dynamic scheduling of demand response reserve
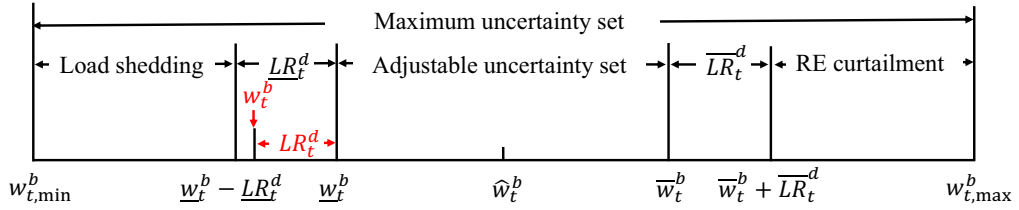
Figure 4: Real-time usage of DR reserve

Since day-ahead DR reserve may not be fully used in real-time operation, the remaining DR reserve can be rescheduled in the following time slots to further reduce the operational risk.

According to the real-time power generation of RE, the actual usage of DR reserve is presented as

$$
LR_t^d = \begin{cases}
-\underline{LR}_t^d & w_{t,\min}^b \leq w_t^b \leq \underline{w}_t^b - \underline{LR}_t^d \\
w_t^b - \underline{w}_t^b & \underline{w}_t^b - \underline{LR}_t^d \leq w_t^b \leq \underline{w}_t^b \\
0 & \underline{w}_t^b \leq w_t^b \leq \overline{w}_t^b \\
w_t^b - \overline{w}_t^b & \overline{w}_t^b \leq w_t^b \leq \overline{w}_t^b + \overline{LR}_t^d \\
\overline{LR}_t^d & \overline{w}_t^b + \overline{LR}_t^d \leq w_t^b \leq w_{t,\max}^b
\end{cases}
\tag{18}
$$

As shown in Fig. 4, in real-time operation, when the actual power output of the RE is within the range of the adjustable uncertainty set $[\underline{w}_t^b, \overline{w}_t^b]$, the DR does not participate in power adjustment, i.e. $LR_t^d = 0$; When the actual power output of the RE is within the set of $[\underline{w}_t^b - \underline{LR}_t^d, \underline{w}_t^b]$, the DR will participate in power adjustment with a value of $w_t^b - \underline{w}_t^b$. In this case, $LR_t^d \leq 0$, which indicates the load is decreased; When the actual power output of RE is within the set of $[\overline{w}_t^b, \overline{w}_t^b + \overline{LR}_t^d]$, the DR will participate in power adjustment with a value of $w_t^b - \overline{w}_t^b$. In this case, $LR_t^d \geq 0$, which

16

indicates the load is increased; When the actual power output of RE is less than $\underline{w}_t^b - \underline{LR}_t^d$ or greater than $\overline{w}_t^b + \overline{LR}_t^d$, the power adjustment is equal to $-\underline{LR}_t^d$ or $\overline{LR}_t^d$ respectively, which are the maximum adjustable amount of DR at time t. Fig. 4 shows the situation when w_t^b is within $[\underline{w}_t^b - \underline{LR}_t^d, \underline{w}_t^b]$.

Since the power adjustment does not necessarily use all planned DR reserve in real-time operation, the dynamic scheduling of DR reserve is proposed in this paper to fully utilize the capacity of DR. The dynamic scheduling of DR reserve is formulated as follows:

$$\min_{\underline{LR}_t^d, \overline{LR}_t^d} \sum_{t=\tau}^{T} (Risk_t^b + C_{ld}\underline{LR}_t^d + C_{li}\overline{LR}_t^d) \tag{19a}$$

$$s.t.\ \forall g \in \mathcal{G}_b, \forall b \in \mathcal{B}, \forall l \in \mathcal{L}, t = \tau, \dots, T$$

$$\sum_{t=\tau}^{T} \overline{LR}_t^d \leq \beta_d - \sum_{t=1}^{\tau-1} LR_t^d \tag{19b}$$

$$\sum_{t=\tau}^{T} \underline{LR}_t^d \leq \beta_d + \sum_{t=1}^{\tau-1} LR_t^d \tag{19c}$$

$$p_{gt}^b = x_{gt}^b + a_{gt}^t \sum_{b \in B}(\hat{w}_t^b - w_t^b) \tag{19d}$$

$$(7a) - (7b), (9), (16e) - (16f) \tag{19e}$$

Constraints (19b) and (19c) indicate the capacity limits of the DR reserve, which are updated according to the actual usage of the DR reserve before the time slot τ. Note that the pre-scheduled power generation x_{gt}^b, participate factor a_{gt}^b, and the lower and upper bounds of the adjustable uncertainty set, i.e. $\underline{w}_t^b$ and $\overline{w}_t^b$, have been solved in the day-ahead scheduling of UC.

The proposed method can provide guidance for system operators to schedule the power system in reducing costs and improving the economy of the power system. In practical implementation, the day-ahead UC scheduling determines the on/off state of the generator, the power output of the generator, the participation factor of the generator, the power dispatch of the DR reserve, and the bounds of the adjustable uncertainty set. In real-time operation, the power output of the generator will be adjusted based on its participation factor to maintain the power balance in the presence of RE forecast error, and the DR reserve is re-dispatched in each time slot to fully utilize its capacity.

17

4. Solution methodology

In this section, the solution methodology is introduced to transfer the UC model (17) into a solvable MILP problem, and the complete process and flowchart of the proposed method are given.

4.1. Transformation of constraints with uncertainties

In this subsection, a detailed process for linearizing the nonlinear constraint with uncertainty is presented. It can be seen from equation (12) that there are nonlinear terms of continuous variable a_{gt}^b and uncertainty variable $w_t^b \in [\underline{w}_t^b, \overline{w}_t^b]$. When equation (12) is substituted into constraints (16a)-(16f), there will be nonlinear terms in constraints (16a)-(16f), which makes (17) an MINLP problem that cannot be solved directly by existing solvers. The linearization method used in Ref. [31] is adopted in this paper to convert the MINLP problem to a solvable MILP problem by introducing auxiliary variables and linear constraints. The linearization of constraint (16e) is taken as an example to show the linearization process of constraints (16a)-(16f).

Firstly, the integer variables are introduced to discrete the continuous variables $\underline{w}_t^b / \overline{w}_t^b$, which are presented as

$$\underline{w}_t^b = \hat{w}_t^b - \underline{M}_t^b \underline{\delta}_t^b \tag{20a}$$

$$\overline{w}_t^b = \hat{w}_t^b + \overline{M}_t^b \overline{\delta}_t^b \tag{20b}$$

$$\underline{\delta}_t^b = (\hat{w}_t^b - w_{t,\min}^b)/N \tag{20c}$$

$$\overline{\delta}_t^b = (w_{t,\max}^b - \hat{w}_t^b)/N \tag{20d}$$

where equations (20c) and (20d) indicate that $[w_{t,\min}^b, \hat{w}_t^b]$ and $[\hat{w}_t^b, w_{t,\max}^b]$ are equally divided into N subintervals, respectively. Equations (20a) and (20b) indicate that the bounds of the adjustable uncertainty set can be expressed as positive and negative deviations from the forecast value of RE. $\underline{M}_t^b$ and $\overline{M}_t^b$ are integer decision variables with a range of $[0, N]$. Therefore, the product of two continuous variables (i.e. a_{gt}^b and $\underline{w}_t^b / \overline{w}_t^b$) is transformed into the product of continuous variable and integer variable (i.e. a_{gt}^b and $\underline{M}_t^b / \overline{M}_t^b$). Equation (16e) is satisfied for any $\forall w_t^b \in [\underline{w}_t^b, \overline{w}_t^b], \forall LR_t^d \in [-\underline{LR}_t^d, \overline{LR}_t^d]$. Since constraint (16e) is linear, the constraint will be satisfied under all possible situations if they hold at the bounds, i.e. $w_t^b = \underline{w}_t^b / \overline{w}_t^b$ and $LR_t^d = -\underline{LR}_t^d / \overline{LR}_t^d$. The situation when $w_t^b = \underline{w}_t^b$ and $LR_t^d = -\underline{LR}_t^d$ is illustrated

as an example to show the process of linearization. Substituting (12) and (20a) in (16e) and considering the case of $w_t^b = \underline{w}_t^b$ and $LR_t^d = -\underline{LR}_t^d$, the expression (21) is obtained.

$$
\sum_{b\in\mathcal{B}} K_l^b(\sum_{g\in\mathcal{G}_b}(x_{gt}^b + a_{gt}^b \sum_{b\in\mathcal{B}} \underline{M}_t^b\underline{\delta}_t^b) - \hat{\varepsilon}_t^b + \hat{w}_t^b - \underline{M}_t^b\underline{\delta}_t^b)
$$
$$
+ \sum_{r\in\mathcal{R}} RE_t^r K_l^r + \sum_{d\in\mathcal{D}} \underline{LR}_t^d K_l^d + C_l \geq 0 \tag{21}
$$

Secondly, the integer variable $\underline{M}_t^b$ is replaced by the sum of a N-dimensional binary vector $\underline{V}_t^b = (\underline{v}_{t1}^b, \ldots, \underline{v}_{tn}^b, \ldots, \underline{v}_{tN}^b)^T$, and the constraint (21) is transformed into

$$
\sum_{b\in\mathcal{B}} K_l^b(\sum_{g\in\mathcal{G}_b}(x_{gt}^b + a_{gt}^b \sum_{b\in\mathcal{B}}\sum_{n=1}^N(\underline{v}_{tn}^b)\underline{\delta}_t^b) - \hat{\varepsilon}_t^b + \hat{w}_t^b - (\sum_{n=1}^N \underline{v}_{tn}^b)\underline{\delta}_t^b)
$$
$$
+ \sum_{r\in\mathcal{R}} RE_t^r K_l^r + \sum_{d\in\mathcal{D}} \underline{LR}_t^d K_l^d + C_l \geq 0 \tag{22}
$$

Thirdly, auxiliary variables $\underline{S}_{gt}^b = (\underline{s}_{gt1}^b, \ldots, \underline{s}_{gtn}^b, \ldots, \underline{s}_{gtN}^b)^T$ and linear constraints (23b)-(23e) are introduced to replace the product of binary and continuous variables (i.e. a_{gt}^b and $\sum_{n=1}^N \underline{v}_{tn}^b$) [46], and the constraint (22) is transformed into

$$
\sum_{b\in\mathcal{B}} K_l^b(\sum_{g\in\mathcal{G}_b}(x_{gt}^b + \sum_{b\in\mathcal{B}}\sum_{n=1}^N(\underline{s}_{gtn}^b)\underline{\delta}_t^b) - \hat{\varepsilon}_t^b + \hat{w}_t^b - (\sum_{n=1}^N \underline{v}_{tn}^b)\underline{\delta}_t^b)
$$
$$
+ \sum_{r\in\mathcal{R}} RE_t^r K_l^r + \sum_{d\in\mathcal{D}} \underline{LR}_t^d K_l^d + C_l \geq 0 \tag{23a}
$$
$$
\underline{s}_{gtn}^b \leq \underline{v}_{tn}^b \tag{23b}
$$
$$
\underline{s}_{gtn}^b \leq a_{gt}^b \tag{23c}
$$
$$
\underline{s}_{gtn}^b \geq a_{gt}^b - (1 - \underline{v}_{tn}^b) \tag{23d}
$$
$$
\underline{s}_{gt}^b \geq 0 \tag{23e}
$$

After transformation, it can be seen that there is no nonlinear term in (23). Linearizing the constraints (16a)-(16d) and (16f) in the same way, the MINLP problem (17) is transformed into a deterministic MILP problem that can be solved directly by existing solvers.
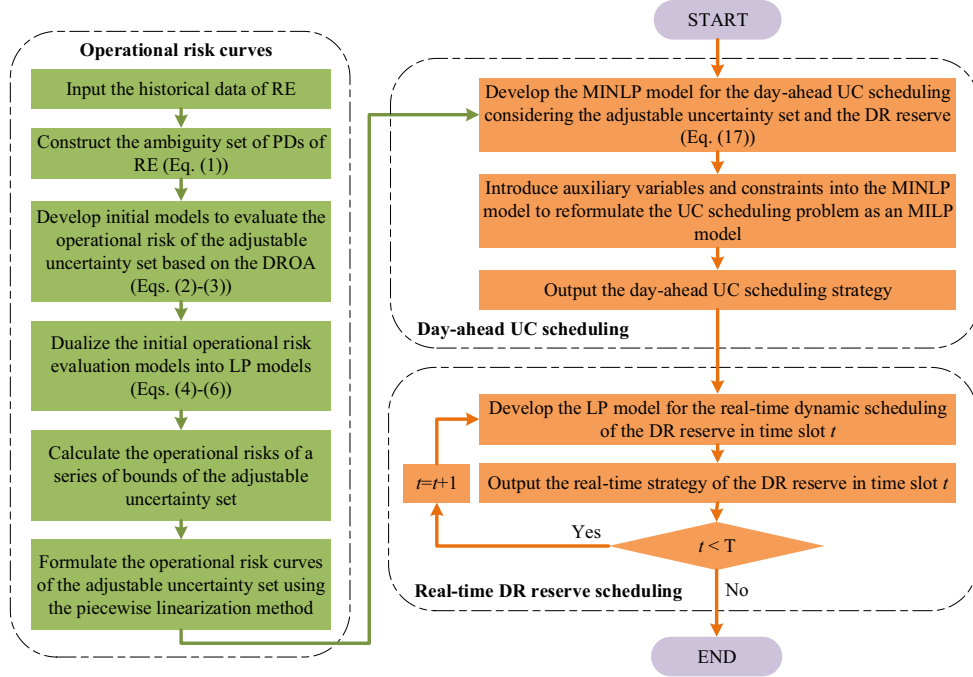
Figure 5: The flowchart of the optimization process

4.2. The complete process of the proposed method

The complete process of the proposed method including the evaluation of the operational risk of the adjustable uncertainty set is summarized in Fig. 5. Firstly, the operational risk curves of the adjustable uncertainty set are calculated by the proposed DROA based on the historical data. Secondly, the day-ahead UC scheduling model is formulated as an MINLP problem, and auxiliary variables and constraints are introduced to transform the original MINLP problem into a solvable MILP problem. Thirdly, the dynamic DR program is formulated as a solvable LP problem.

5. Simulation results

Three case studies including the IEEE 6-bus, 30-bus, and 118-bus systems are performed to verify the effectiveness of the proposed approach. It is noted that these systems are standard test systems for operation of power system. All the simulations are programmed in MATLAB with YALMIP [47] as the modelling tool and Gurobi as the solver running on a Win 7 PC with a 3.4 GHz CPU and 16 GB RAM. The MILP problem and LP problems are solved in the Gurobi solver by the branch-and-cut algorithm [48] and simplex algorithm [49], respectively.
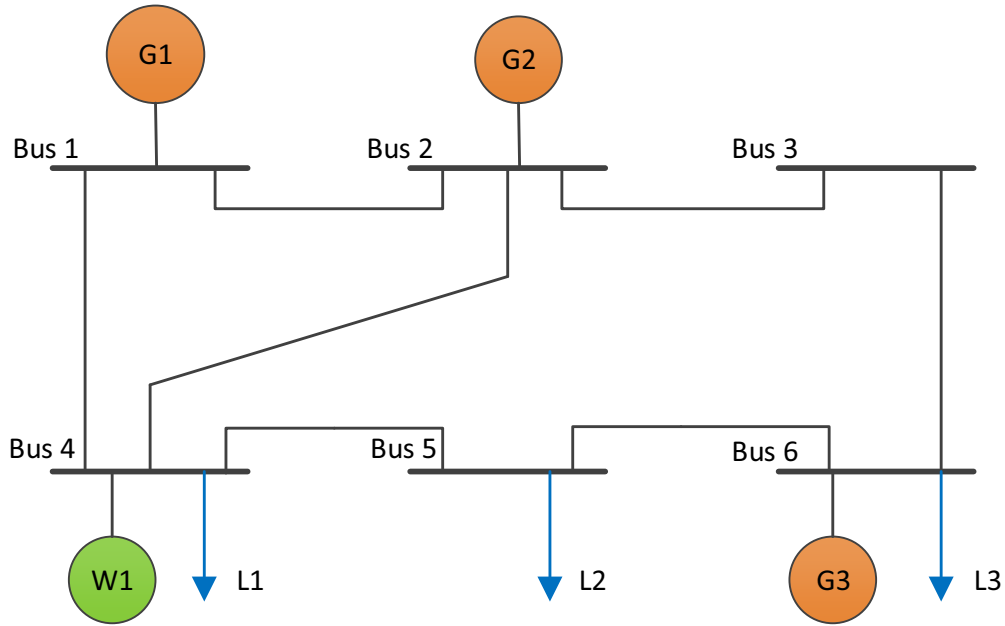
Figure 6: Diagram of 6-bus test system

5.1. Case study of a 6-bus system

Firstly, the system description of the 6-bus system is presented. Then the operational risk curves of the adjustable uncertainty are shown to verify the superiority of the proposed DROA-based operational risk evaluation method. Based on the operational risk curves, simulation results of the proposed UC with the consideration of the adjustable uncertainty set are presented. The comparison between the proposed method and other methods is shown to demonstrate the effectiveness of the proposed method. Finally, the sensibility of the capacity of the DR reserve is presented to investigate the influence of the DR reserve capacity on the proposed method.

5.1.1. System description

The diagram of the 6-bus test system is shown in Fig. 6. There is a wind farm at bus 4 with a capacity of 40MW, and the load at bus 4 participates in DR. Detailed network data of the 6-bus system refers to [50, 51]. The percentage profiles of the load and the wind power output are shown in Fig. 7. The load is equal to the multiplication of the percentage and the load data given in [51], and the wind power output is equal to the multiplication of the percentage and the wind farm capacity. Incentive prices for DR reserve of load decrease and load increase are both \$1.1/MWh [52]. Based on Weibull

distribution, historical data of wind power is generated, and the ambiguity sets $\mathcal{P}_t^{ls}$ and $\mathcal{P}_t^{rc}$ are constructed according to the generated data. It should be noted that the Weibull distribution is only used to generate the historical data and the proposed method does not require the knowledge of the PD of wind power. The penalty prices for load shedding and wind curtailment are $500/MWh and $50/MWh [43], respectively.
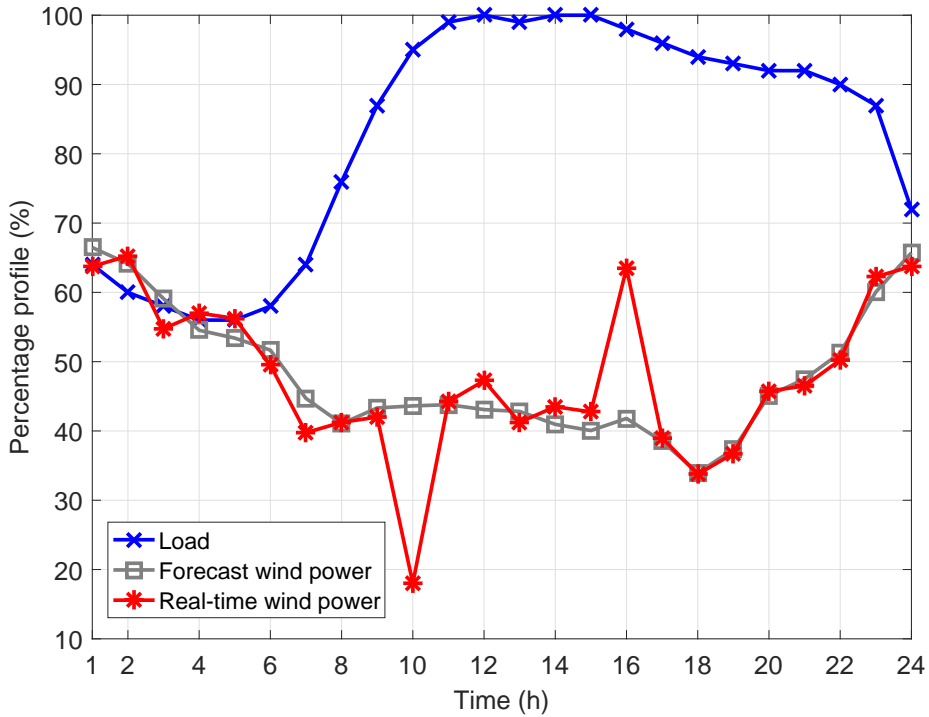

Figure 7: Data of load and wind power

5.1.2. Comparison of operational risk curves

Two different evaluation methods of operational risk are investigated in this paper, namely the worst risk approach (WRA) in [31] and the proposed DROA. In WRA, the operational risk is calculated by the maximum deviation between the adjustable uncertainty set and the maximum uncertainty set, i.e. $Risk_t^b = \max\{C_{ls}(\underline{w}_t^b - w_{t,\min}^b), C_{rc}(w_{t,\max}^b - \overline{w}_t^b)\}$. Two situations of DROA with less and more probabilistic information named DROA1 and DROA2 are considered. In DROA1 and DROA2, the operational risks are calculated by (2) and (3). The difference between DROA1 and DROA2 is that the probabilistic information of the ambiguity set in DROA1 is more than that in DROA2. For the load shedding risk, as shown in Fig. 2, the ambiguity set

22

of DROA1 is constructed by the probabilistic information of intervals $W_i, i = 1, 2, \ldots, m$ and $[\underline{w}_t^b, w_{max}^b]$ while the ambiguity set of DROA2 is constructed by the probabilistic information of only two intervals $[w_{min,t}^b, \underline{w}_t^b]$ and $[\underline{w}_t^b, w_{max}^b]$. So is the case for the RE curtailment risk.

The operational risk curves of the two methods in the first time slot are presented in Fig. 8. The operational risks of load shedding and RE curtailment in WRA are larger than that in DROA1 and DROA2. Moreover, the DROA1 obtains smaller operational risks of load shedding and RE curtailment in comparison with DROA2. It is because more probabilistic information of RE is utilized in DROA1, and its conservativeness of the operational risk evaluation is reduced. In conclusion, the proposed DROA1 obtains the least conservativeness of the operational risk compared with other methods.
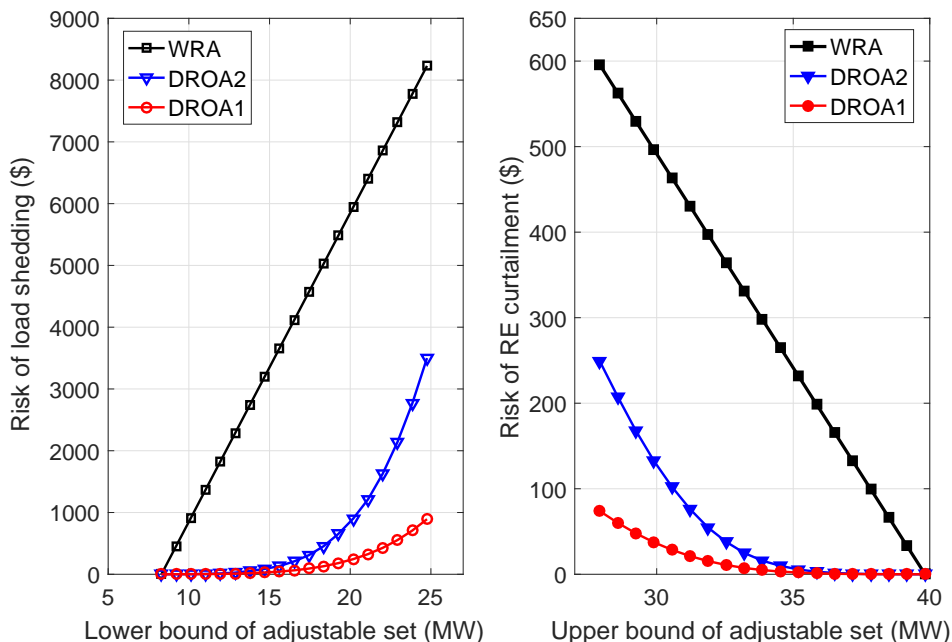
Figure 8: Operational risk curves with different methods

5.1.3. Simulation results of the proposed method

It is assumed that $\underline{LR}_{max}^4 = \overline{LR}_{max}^4 = 3$MW and $\beta_4 = 18$MWh in the 6-bus system [31]. The simulation results of the 6-bus system are shown in Figs. 9-13. Fig. 9 shows the on/off states of the generators. In Fig. 9, the yellow color indicates that the generator is on while the green color indicates that the generator is off. Fig. 10 and Fig. 11 show the day-ahead power

23

outputs and the participation factors of the generators, respectively. In real-time operation, the generators will adjust their power outputs according to the participation factors shown in Fig. 11 to ensure the power balance under the wind power uncertainty. Fig. 12 shows the day-ahead scheduling of DR reserve. Fig. 13 shows the adjustable uncertainty set of the wind farm at bus 4. The lower and upper bounds of the maximum uncertainty set are obtained from historical data.
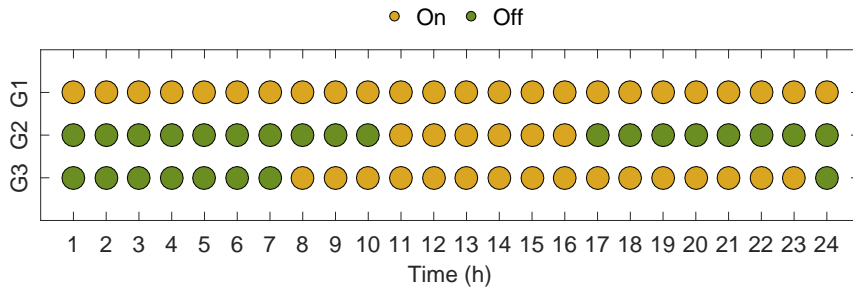

Figure 9: On/off states of the generators
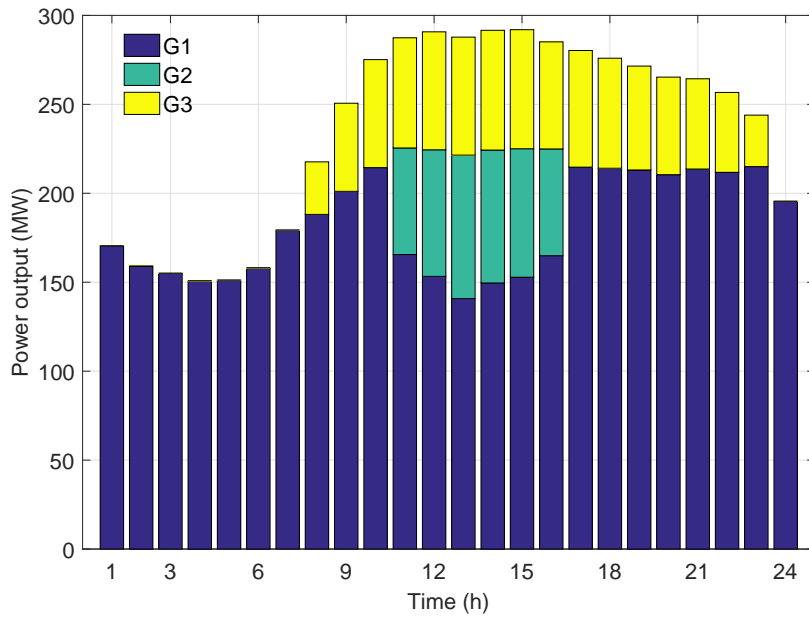
Figure 10: Power outputs of the generators
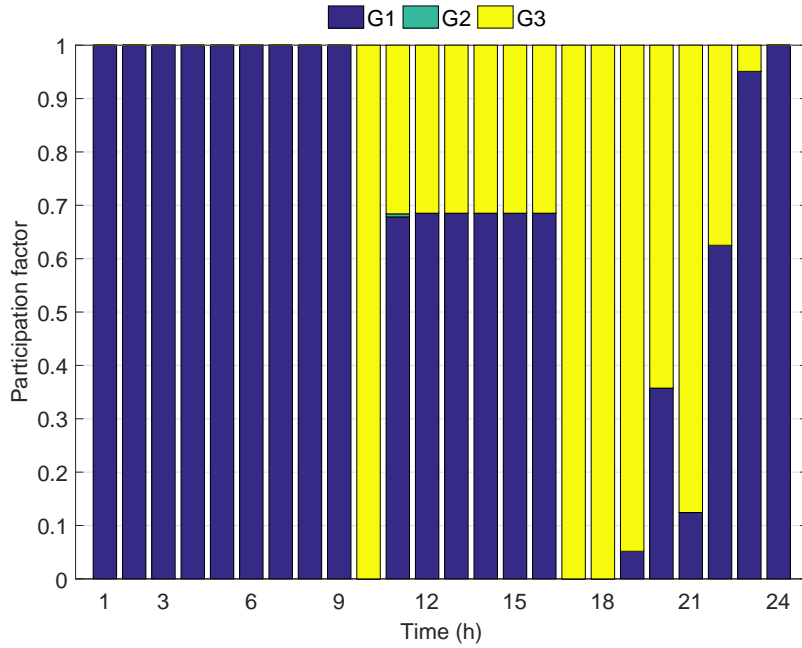
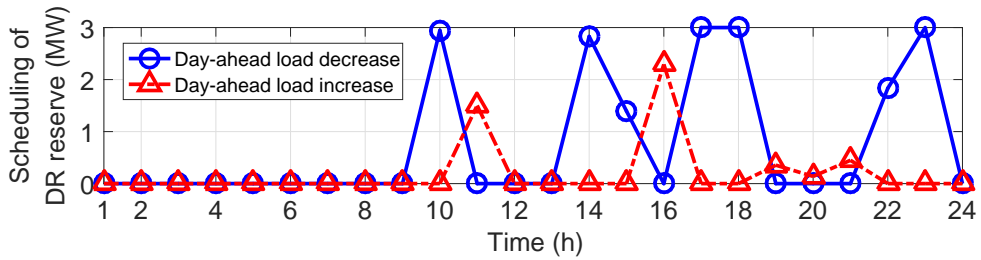Figure 11: Participation factors of the generators

Figure 12: Day-ahead scheduling of DR reserve

To verify the effectiveness of the dynamic scheduling of DR reserve, a real-time power output of RE shown in Fig. 7 is assumed. Simulation results of the dynamic scheduling of DR reserve and actual usage of DR reserve in a day are shown in Fig. 14.
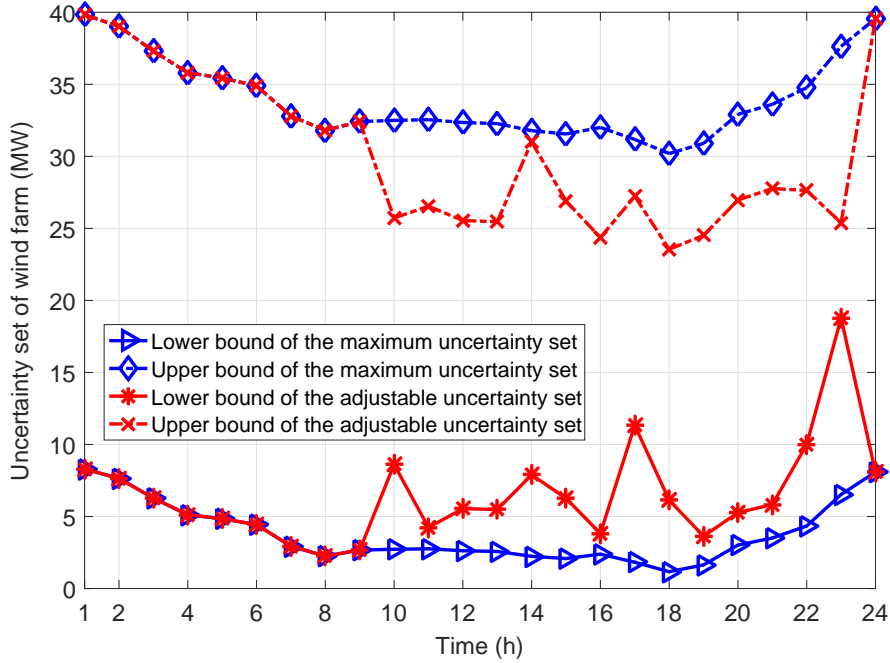
Figure 13: Adjustable uncertainty set of wind farm

It can be seen from Fig. 14(b) and Fig. 12 that the actual usage of the DR reserve is less than the pre-scheduled amount in day-ahead scheduling. The remaining capacity of the DR reserve is rescheduled in the following time slots. Comparing Fig. 14(a) with Fig. 12, the DR reserve of load decrease from $t = 12$ to $t = 15$ and $t = 22$ is increased from 0 MW, 0 MW, 2.83 MW, 1.39 MW, and 1.83 MW in day-ahead scheduling to 0.11 MW, 0.39 MW, 3 MW, 2.78 MW, and 3 MW in dynamic scheduling. For DR reserve of load increase in dynamic scheduling, its value at time slot $t = 22$ is also increased from 0 MW to 1.65 MW. With the dynamic scheduling of DR reserve, the total operational risk of the power system is decreased from $243.03 in day-ahead scheduling to $227.83 in dynamic scheduling. In conclusion, the dynamic scheduling of DR reserve helps reduce the operational risk of the power system.

5.1.4. The comparison between the proposed method and other methods

The proposed method is compared with other methods to test its effectiveness, and the description of these methods is shown in Table 1. Based
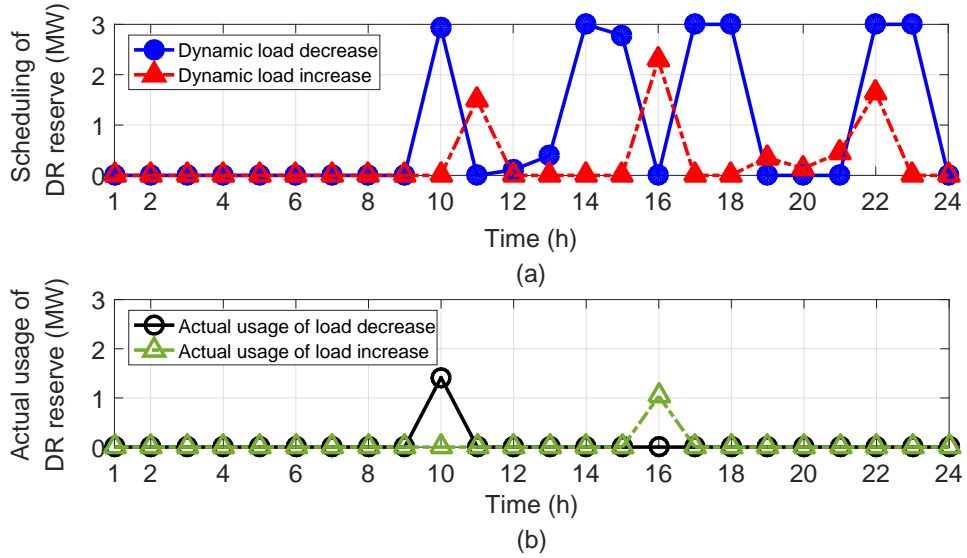
26

Figure 14: (a) Dynamic scheduling of DR reserve (b) Actual usage of DR reserve

on the operational risk curves shown in Fig. 8, M-DROA1 is the proposed method with the operational risk curve of DROA1, and M-WRA adopts the operational risk curve of WRA. M-ROA is the benchmark case, which is based on the traditional ROA. Since M-ROA considers the maximum uncertainty set of RE in UC scheduling, there is no operational risk. Simulation results of the three methods are shown in Table 2. The objective function value of the M-DROA1 is the smallest while the M-ROA is the largest. Since M-ROA is based on ROA which requires all constraints to be satisfied within the maximum uncertainty set of RE, it is the most conservative method in comparison with other methods. Since M-WRA considers the maximum operational risk of the bounds of the adjustable uncertainty set, its total cost is the second largest.

Table 1: Description of three methods

Method	Operational risk curve
M-DROA1	DROA1
M-WRA	WRA
M-ROA	N/A

27

Table 2: Comparison among three methods on the 6-bus system

Method	Objective value (10^5 \$)
M-DROA1	1.3833
M-WRA	1.3945
M-ROA	1.4093

5.1.5. Sensibility of the capacity of demand response reserve

The simulation results of different capacities of DR reserve in M-DROA1 are shown in Fig. 15. It can be observed that the total cost of the power system decreases with the increase of DR reserve capacity. When there is no DR reserve, i.e. $\overline{LR}_{\max}^4 = \underline{LR}_{\max}^4 = \beta_4 = 0$, as shown in Table 3, the total cost of the power system is $\$1.3883 \times 10^5$, while the total cost is $\$1.3833 \times 10^5$ when the capacity of DR reserve is $\underline{LR}_{\max}^4 = \overline{LR}_{\max}^4 = 3$MW and $\beta_4 = 18$MWh. It demonstrates that DR reserve plays an important role in reducing the total cost.
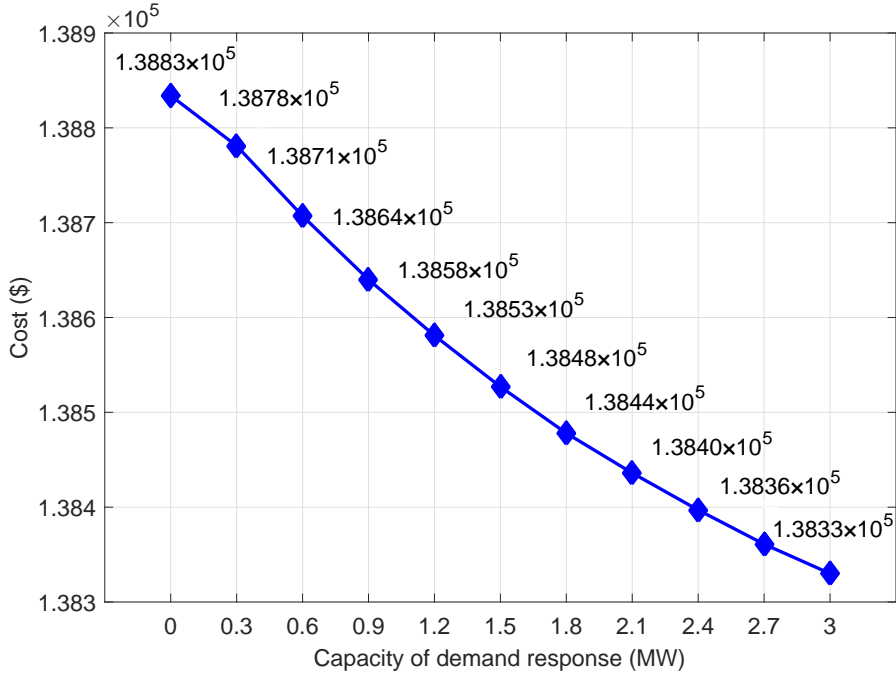

Figure 15: Sensibility of the capacity of DR reserve

Table 3: Comparison of objective values between situations with and without DR reserve on 6-bus system

Objective value	With DR reserve	Without DR reserve
6-bus system (10^5 \$)	1.3833	1.3883

5.2. Case studies of 30-bus and 118-bus systems

The proposed method is tested on the 30-bus and 118-bus systems to further verify its effectiveness. The details of the test systems refer to [51]. It is assumed that $\underline{LR}^7_{\max} = \overline{LR}^7_{\max} = 3.5\text{MW}$ and $\beta_7 = 10\text{MWh}$ for 30-bus system [31]. For 118-bus system, $\underline{LR}^{36}_{\max} = \overline{LR}^{36}_{\max} = \underline{LR}^{77}_{\max} = \overline{LR}^{77}_{\max} = 5\text{MW}$ and $\beta_{36} = \beta_{77} = 20\text{MWh}$. The comparison of the three methods is shown in Table 4, and the UC solution of M-DROA1 is shown in Ref. [51]. By introducing the adjustable uncertainty set and considering probabilistic information when evaluating operational risks, the proposed M-DROA1 reduces the total cost of UC and operational risk compared with other methods.

Table 4: Comparison of objective values among different methods on 30-bus and 118-bus systems

Method	30-bus system (10^5 \$)	118-bus system (10^6 \$)
M-DROA1	1.3849	1.4042
M-WRA	1.3925	1.4054
M-ROA	1.4055	1.4067

The simulation results of the 30-bus and 118-bus systems obtained by M-DROA1 with and without considering the DR reserve are shown in Table 5. It can be observed from the Table 5 that the total cost of the power system is effectively reduced by the participation of the DR reserve.

Table 5: Comparison of objective values between situations with and without DR reserve on 30-bus and 118-bus systems

Objective value	With DR reserve	Without DR reserve
30-bus system (10^5 \$)	1.3849	1.3870
118-bus system (10^6 \$)	1.4042	1.4052

The simulation results of the day-ahead scheduling of DR reserve, dynamic scheduling of DR reserve, and actual usage of DR reserve for the 30-bus and 118-bus systems are shown in Fig. 16 and Fig. 17, respectively. It can be seen from Fig. 16 and Fig. 17 that the dynamic DR reserve is rescheduled in real-time operation.

For the 30-bus system, it can be seen from Fig. 16(c) that the actual usage of the DR reserve in real-time operation is less than their pre-scheduled amount in day-ahead scheduling. Comparing Fig. 16(a) and Fig. 16(b), the

DR reserve of load decrease at $t = 11$, $t = 16$ and $t = 22$ is increased from 0 MW, 0 MW and 2.38 MW in day-ahead scheduling to 0.06 MW, 0.11 MW and 2.91 MW in dynamic scheduling. Besides, the DR reserve of load increase at $t = 16$ and $t = 22$ is increased from 1.77 MW and 0 MW in day-ahead scheduling to 1.97 MW and 0.77 MW in dynamic scheduling. Because of the introduction of the dynamic DR, the operational risk of the 30-bus system is reduced from \$65.17 in day-ahead scheduling to \$62.17 in dynamic scheduling.
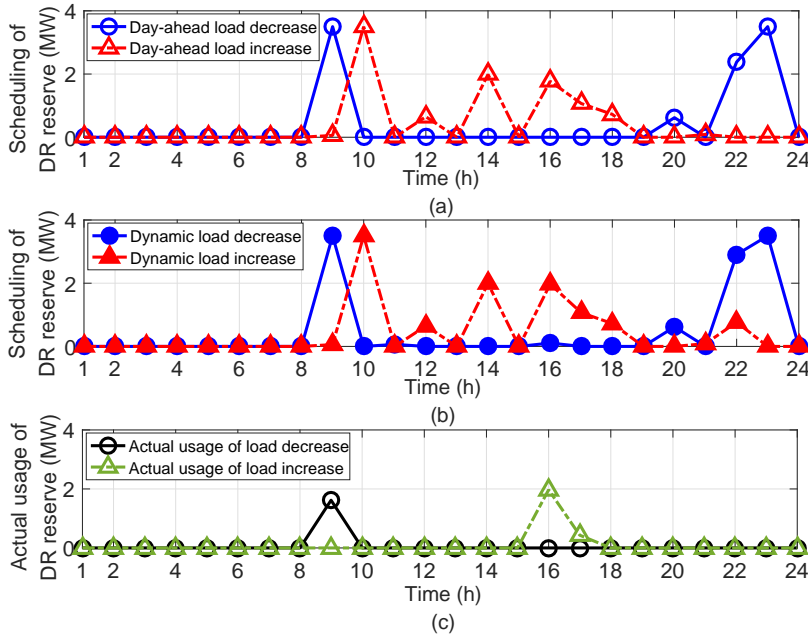

Figure 16: (a) Day-ahead scheduling of DR reserve (b) Dynamic scheduling of DR reserve (c) Actual usage of DR reserve

For the 118-bus system, it can be seen from Fig. 17(c1) and Fig. 17(c2) that the actual usage of the DR reserve 1 and DR reserve 2 in real-time operation is less than their pre-scheduled amount in day-ahead scheduling. Comparing Fig. 17(a1) and Fig. 17(b1), the DR reserve 1 of load decrease from $t = 13$ to $t = 16$, $t = 18$, and $t = 23$ is increased from 3.43 MW, 0 MW, 0.37 MW, 3.38 MW, 4.38 MW and 0 MW in day-ahead scheduling to 5 MW, 1.17 MW ,1.88 MW, 3.57 MW, 5 MW and 0.09 MW in dynamic scheduling. The DR reserve 1 of load increase at $t = 16$ is increased from 4.72 MW in day-ahead scheduling to 5 MW in dynamic scheduling. Similarly, comparing

Fig. 17(a2) and Fig. 17(b2), the DR reserve 2 of load decrease from $t = 14$ to $t = 16$, $t = 18$, and $t = 23$ is increased from 0 MW, 4.93 MW, 3.38 MW, 1.27 MW and 0 MW in day-ahead scheduling to 2.14 MW, 5 MW, 4.54 MW, 2.92 MW and 2.07 MW in dynamic scheduling. The DR reserve 2 of load increase at $t = 16$ and $t = 23$ is increased from 2.87 MW and 0 MW in day-ahead scheduling to 5 MW and 1.58 MW in dynamic scheduling. Due to the use of the dynamic DR, the operational risk of the 118-bus system is reduced from $201.03 in day-ahead scheduling to $165.98 in real-time operation.

6. Conclusion

In this paper, the adjustable uncertainty set and the DR program are combined to address the uncertainty of RE in UC. A DROA is adopted to evaluate the operational risks of load shedding and RE curtailment that are caused by the adjustable uncertainty set. Based on the evaluation of the operational risk, the bounds of the adjustable uncertainty set and the day-ahead scheduling of the DR program are determined to reduce the cost of UC and the operational risk. This risk is further reduced by the dynamic DR program in real-time operation. From simulation results, the following conclusions can be drawn:

- The proposed DROA is less conservative to evaluate the operational risk of the adjustable uncertainty set, and the conservativeness of the evaluation of the operational risk decreases with more probabilistic information of uncertain RE taken into account.

- Based on the operational risk evaluated by the DROA, the proposed UC scheduling with the consideration of the adjustable uncertainty set and the DR program reduces the cost of UC in comparison with other methods.

- By fully utilizing the capacity of DR, the dynamic DR program further reduces the operational risk in comparison with the static DR program.

In our future work, the adjustable uncertainty set for multiple RE considering their correlations will be investigated. Moreover, the adjustable uncertainty set will be generalized to the integrated energy system to investigate the uncertainty of different energy sources.
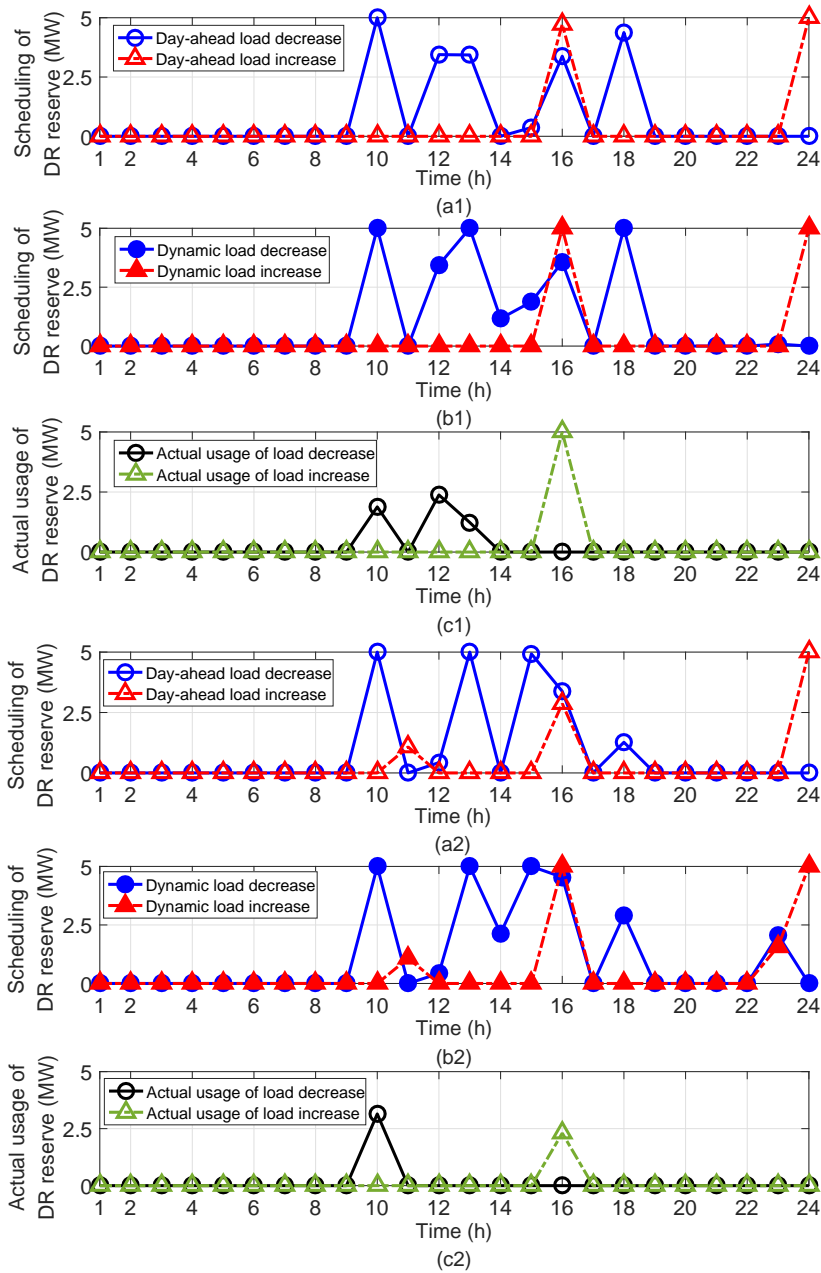
Figure 17: (a1) Day-ahead scheduling of DR reserve 1 (b1) Dynamic scheduling of DR reserve 1 (c1) Actual usage of DR reserve 1 (a2) Day-ahead scheduling of DR reserve 2 (b2) Dynamic scheduling of DR reserve 2 (c2) Actual usage of DR reserve 2

32

Reference

[1] R. Han, J. Li, Z. Guo, Optimal quota in China's energy capping policy in 2030 with renewable targets and sectoral heterogeneity, Energy (2021) 121971.

[2] N. G. Cobos, J. M. Arroyo, N. Alguacil, A. Street, Network-constrained unit commitment under significant wind penetration: A multistage robust approach with non-fixed recourse, Appl. Energy 232 (2018) 489–503.

[3] H. Abdi, Profit-based unit commitment problem: A review of models, methods, challenges, and future directions, Renew. Sustain. Energy Rev. 138 (2021) 110504.

[4] M. Vatanpour, A. Sadeghi Yazdankhah, The impact of energy storage modeling in coordination with wind farm and thermal units on security and reliability in a stochastic unit commitment, Energy 162 (2018) 476–490.

[5] M. H. Shams, M. Shahabi, M. MansourLakouraj, M. Shafie-khah, J. P. Catalão, Adjustable robust optimization approach for two-stage operation of energy hub-based microgrids, Energy 222 (2021) 119894.

[6] M. Shahbazitabar, H. Abdi, A novel priority-based stochastic unit commitment considering renewable energy sources and parking lot cooperation, Energy 161 (2018) 308–324.

[7] Q. Wang, Y. Guan, J. Wang, A chance-constrained two-stage stochastic program for unit commitment with uncertain wind power output, IEEE Trans. Power Syst. 27 (1) (2012) 206–215.

[8] S. Mohammadi, S. Soleymani, B. Mozafari, Scenario-based stochastic operation management of microgrid including wind, photovoltaic, micro-turbine, fuel cell and energy storage devices, Int. J. Electr. Power Energy Syst. 54 (2014) 525–535.

[9] A. Baharvandi, J. Aghaei, T. Niknam, M. Shafie-Khah, R. Godina, J. P. S. Catalão, Bundled generation and transmission planning under demand and wind generation uncertainty based on a combination of

robust and stochastic optimization, IEEE Trans. Sustain. Energy 9 (3) (2018) 1477–1486.

[10] C. Ozay, M. Celiktas, Stochastic optimization energy and reserve scheduling model application for alaçatı, Turkey, Smart Energy 3 (2021) 100045.

[11] T. Ding, C. Li, Y. Yang, J. Jiang, Z. Bie, F. Blaabjerg, A two-stage robust optimization for centralized-optimal dispatch of photovoltaic inverters in active distribution networks, IEEE Trans. Sustain. Energy 8 (2) (2017) 744–754.

[12] M. S. Pinto, V. Miranda, O. R. Saavedra, Risk and unit commitment decisions in scenarios of wind power uncertainty, Renew. Energy 97 (2016) 550–558.

[13] S.-E. Razavi, A. Esmaeel Nezhad, H. Mavalizadeh, F. Raeisi, A. Ahmadi, Robust hydrothermal unit commitment: A mixed-integer linear framework, Energy 165 (2018) 593–602.

[14] C. He, L. Wu, T. Liu, W. Wei, C. Wang, Co-optimization scheduling of interdependent power and gas systems with electricity and gas uncertainties, Energy 159 (2018) 1003–1015.

[15] D. Testi, L. Urbanucci, C. Giola, E. Schito, P. Conti, Stochastic optimal integration of decentralized heat pumps in a smart thermal and electric micro-grid, Energy Convers. Manage. 210 (2020) 112734.

[16] R. Jiang, J. Wang, Y. Guan, Robust unit commitment with wind power and pumped storage hydro, IEEE Trans. Power Syst. 27 (2) (2012) 800–810.

[17] J. Yi, P. F. Lyons, P. J. Davison, P. Wang, P. C. Taylor, Robust scheduling scheme for energy storage to facilitate high penetration of renewables, IEEE Trans. Sustain. Energy 7 (2) (2016) 797–807.

[18] C. Zhao, Y. Guan, Unified stochastic and robust unit commitment, IEEE Trans. Power Syst. 28 (3) (2013) 3353–3361.

[19] Y. Zhang, Y. Liu, S. Shu, F. Zheng, Z. Huang, A data-driven distributionally robust optimization model for multi-energy coupled system

considering the temporal-spatial correlation and distribution uncertainty of renewable energy sources, Energy 216 (2021) 119171.

[20] G. A. Hanasusanto, V. Roitch, D. Kuhn, W. Wiesemann, A distributionally robust perspective on uncertainty quantification and chance constrained programming, Math. Program. 151 (1) (2015) 35–62.

[21] X. Zheng, H. Chen, Y. Xu, Z. Li, Z. Lin, Z. Liang, A mixed-integer SDP solution to distributionally robust unit commitment with second order moment constraints, CSEE J. Power Energy Syst. 6 (2) (2020) 374–383.

[22] P. Xiong, P. Jirutitijaroen, C. Singh, A distributionally robust optimization model for unit commitment considering uncertain wind power generation, IEEE Trans. Power Syst. 32 (1) (2017) 39–49.

[23] C. Wang, F. Liu, J. Wang, W. Wei, S. Mei, Risk-based admissibility assessment of wind generation integrated into a bulk power system, IEEE Trans. Sustain. Energy 7 (1) (2016) 325–336.

[24] C. Wang, F. Liu, J. Wang, F. Qiu, W. Wei, S. Mei, S. Lei, Robust risk-constrained unit commitment with large-scale wind generation: An adjustable uncertainty set approach, IEEE Trans. Power Syst. 32 (1) (2017) 723–733.

[25] C. Shao, X. Wang, M. Shahidehpour, X. Wang, B. Wang, Security-constrained unit commitment with flexible uncertainty set for variable wind power, IEEE Trans. Sustain. Energy 8 (3) (2017) 1237–1246.

[26] L. Yao, X. Wang, C. Duan, J. Guo, X. Wu, Y. Zhang, Data-driven distributionally robust reserve and energy scheduling over wasserstein balls, IET Gener. Transm. Distrib. 12 (1) (2018) 178–189.

[27] Z. Guo, W. Wei, L. Chen, M. Shahidehpour, S. Mei, Economic value of energy storages in unit commitment with renewables and its implication on storage sizing, IEEE Trans. Sustain. Energy 12 (4) (2021) 2219–2229.

[28] M. Daraei, P. E. Campana, E. Thorin, Power-to-hydrogen storage integrated with rooftop photovoltaic systems and combined heat and power plants, Appl. Energy 276 (2020) 115499.

[29] R. Bahmani, H. Karimi, S. Jadid, Stochastic electricity market model in networked microgrids considering demand response programs and renewable energy sources, Int. J. Electr. Power Energy Syst. 117 (2020) 105606.

[30] D. Pozo, J. Contreras, E. E. Sauma, Unit commitment with ideal and generic energy storage units, IEEE Trans. Power Syst. 29 (6) (2014) 2974–2984.

[31] Y. Du, Y. Li, C. Duan, H. B. Gooi, L. Jiang, Adjustable uncertainty set constrained unit commitment with operation risk reduced through demand response, IEEE Trans. Ind. Informat. 17 (2) (2021) 1154–1165.

[32] Y. Zhou, M. Shahidehpour, Z. Wei, Z. Li, G. Sun, S. Chen, Distributionally robust unit commitment in coordinated electricity and district heating networks, IEEE Trans. Power Syst. 35 (3) (2020) 2155–2166.

[33] M. Elsisi, New design of robust PID controller based on meta-heuristic algorithms for wind energy conversion system, Wind Energy 23 (2) (2020) 391–403.

[34] M. Ismail, A. Bendary, M. Elsisi, Optimal design of battery charge management controller for hybrid system PV/wind cell with storage battery, Int. J. Power Energy Convers. 11 (2020) 412.

[35] J. Khorasani, A new heuristic approach for unit commitment problem using particle swarm optimization, Arab J. Sci. Eng. 37 (4) (2012) 1033–1042.

[36] M. Elsisi, H. Abdelfattah, New design of variable structure control based on lightning search algorithm for nuclear reactor power system considering load-following operation, Nucl. Eng. Technol. 52 (3) (2020) 544–551.

[37] M. Elsisi, New variable structure control based on different meta-heuristics algorithms for frequency regulation considering nonlinearities effects, Int. Trans. Electr. Energy Syst. 30 (7) (2020) e12428.

[38] A. Frangioni, C. Gentile, F. Lacalandra, Sequential Lagrangian-MILP approaches for unit commitment problems, Int. J. Electr. Power Energy Syst. 33 (3) (2011) 585–593.

[39] B. Zeng, L. Zhao, Solving two-stage robust optimization problems using a column-and-constraint generation method, Oper. Res. Lett. 41 (5) (2013) 457–461.

[40] J. Alemany, F. Magnago, Benders decomposition applied to security constrained unit commitment: Initialization of the algorithm, Int. J. Electr. Power Energy Syst. 66 (2015) 53–66.

[41] GUROBI, GUROBI Optimizer [Online]. Available: `https://www.gurobi.com`.

[42] H. Wu, M. Shahidehpour, A. Alabdulwahab, A. Abusorrah, Thermal generation flexibility with ramping costs and hourly demand response in stochastic security-constrained scheduling of variable energy sources, IEEE Trans. Power Syst. 30 (6) (2015) 2955–2964.

[43] C. Duan, L. Jiang, W. Fang, J. Liu, Data-driven affinely adjustable distributionally robust unit commitment, IEEE Trans. Power Syst. 33 (2) (2018) 1385–1398.

[44] Y. Zhang, S. Shen, J. L. Mathieu, Distributionally robust chance-constrained optimal power flow with uncertain renewables and uncertain reserves provided by loads, IEEE Trans. Power Syst. 32 (2) (2017) 1378–1388.

[45] C. Wang, X. Li, Y. Zhang, Y. Dong, X. Dong, M. Wang, Two stage unit commitment considering multiple correlations of wind power forecast errors, IET Renew. Power Gener. 15 (3) (2021) 574–585.

[46] J. Bisschop, AIMMS - Optimization Modeling, Paragon Decision Technology, 2012.

[47] J. Lofberg, Yalmip : a toolbox for modeling and optimization in matlab, in: 2004 IEEE International Symposium on Computer Aided Control Systems Design, 2004, pp. 284–289.

[48] J. E. Mitchell, Branch and Cut, John Wiley & Sons, Ltd, 2011.

[49] M. Bazaraa, J. Jarvis, H. Sherali, Linear Programming and Network Flows, John Wiley & Sons, Ltd, 2009.

[50] MATPOWER, Free, open-source Electric Power System Simulation and Optimization Tools for MATLAB and Octave [Online]. Available: `http://www.pserc.cornell.edu/matpower/`.

[51] K. Qing, Data and simulation results of 6-bus, 30-bus and 118-bus systems [Online]. Available: `https://www.researchgate.net/profile/Ke_Qing/publications`.

[52] M. Vrakopoulou, J. L. Mathieu, G. Andersson, Stochastic optimal power flow with uncertain reserves from demand response, in: 2014 47th Hawaii International Conference on System Sciences, 2014, pp. 2353–2362.